13

Modelling of polymeric fibre-composites and finite element simulation of mechanical properties

Robert A. Shanks
CRC for Polymers, Applied Sciences, RMIT University
GPO Box 2476V Melbourne Victoria
Australia
robert.shanks@rmit.edu.au

Summary
Polymer composites are formed as random or anisotropic fibre dispersions, sheets with long fibre felted or woven fabrics and laminates of such sheets. A thermoset polymer in liquid form is mixed with the fibres and then cured. Thermoplastics must be intermingled with the fabric and the matrix phase united by melting of the thermoplastic and compaction of the composition. The composite sheets are thermoformable by virtue of the thermoplastic matrix phase. These composites present many compositional, structural and processing variables that contribute to properties. These composites are less uniform than typical thermoset resin composites where fibres are wet with a liquid resin that is then solidified by chain extension and crosslinking. Typical characterisation and mechanical performance tests are available to investigate and optimise the composites. Finite element analysis (FEA) enables a theoretical approach to understanding of the structure–property relationships and confirmation of interpretation of measured properties. A displacement field is suited to identifying and quantifying stress intensities in local regions of the composite to determine parameters critical to the performance of the composites. This chapter reviews the application of FEA to various composite types, stress situations and failure mechanisms. The FEA model design and simulation method are evaluated and compared.

1. Introduction

1.1 Types of composite

Composites based upon thermoplastics such as polypropylenes, polyethylenes, poly(ethylene terephthalate), poly(butylene terephtahate), various polyamides, polystyene and its copolymers with butadiene and acrylonitrile, poly(vinyl chloride) thermoplastic polyurethanes, thermoplastic elastomers and biopolyesters such as poly(lactic acid), poly(hydroxybutyrate) and its copolymers with hydroxyvaleric acid. Thermosetting polymers include epoxy resins, unsaturated polyesters, vinyl esters, epoxy-acrylates, polyurethanes, polyisocyanurates, polybismaleimides, polysiloxanes, formaldehyde based

resins such as phenolic, melamine and urea, and many synthetic elastomers. Epoxy resins are the most commonly studied polymers using finite element methods and they are frequently cited as examples in this chapter.

Fibrous reinforcements include cellulosic fibres such as flax, hemp and others, glass fibres, carbon fibres, mineral fibres, synthetic fibres related to the matrix polymer. Table 1 shows Common fibre reinforcements with brief comments. Short fibres are chosen for direct addition to a polymer in extrusion or injection moulding. Common short fibres are chopped glass and carbon fibres, wood flour and other plant derived cellulosic fibres. Long fibres may be used in pultrusion, woven mats or felted (non-woven such as prepared by needle punching) mats. Mats require inclusion of polymer so that composites can be prepared by thermoforming since the structure of the mat must be maintained. Nano-fibres are subject to much recent investigation and they are of increasing commercial importance, such as carbon nano-tubes, microcrystalline cellulose or nano-cellulose, boron nitride and alumina whiskers. The composites discussed mainly include fibres, however other fillers such a glass spheres and particulate or platelet shapes are studied using FEA since they can be represented in two- or three-dimensional models of polymer composites. Polymer can be included as another fibre or as a powder, that are subsequently melted to form a uniform matrix between and around fibres, as a plastisol (polymer dispersed in plasticiser) that is thermally gelled to form a solid matrix, or as a chain-extendable or cross-linking pre-polymer. Sometimes a third component is included as an interphase surrounding the dispersed phase or when the layers of a laminate have different properties. A more complex model may include a density gradient within the matrix, often to distinguish surface layers from the interior.

Fibre	Composition	Description
Glass fibre	E-glass or S-glass	Chemically resistant, with size coating, need coupling agent
Carbon fibre	Graphite (formed by polymer pyrolysis)	High modulus and strength
Carbon nanotubes	Graphite cylinders	High modulus, strength, conductivity
Kevlar	Poly(phenylene terephthalamide)	High modulus / high strength types
Bast fibre (hemp, flax, rami)	Cellulose	Native or textile crystals, moisture sensitive, long fibres can be woven
Wood fibre or flour	Cellulose	As above, short fibres
Nano-cellulose	Partially hydrolysed cellulose	Crystalline perfection, high properties
Polymer fibres	Polypropylene, Polyamides, poly(ethylene terephthalate)	Moderate modulus and strength, used in special purpose composites
Mineral fibres	Rock wool, boron nitride, alumina	High performance

Table 1. Fibres for reinforcement of polymer composites

The thermoplastic composites under consideration contain long fibres that are structured by felting, typically using a needle-punch method, or woven. The composites are planar, with application as sheets or panelling, such as in automotive liner use or in building panels. The composite sheets are thermo-formable because the matrix is a thermoplastic. In automotive application they are formed into the many complex shapes required by the interior shape and contours. Fibre weave and/or entanglement will increase tensile strength across the plane of the composite. Fibres crossing the plane in either felted or woven composites can increase the interlayer strength thus preventing peeling of layers from sheets. The composite sheets can be laminates with one or two decorative or protective layers. In automotive use the lamination is typically an upholstered, leather-like or wood-like finish. The thermosetting composites may be readily formed into any shape, however the shape cannot be changed after formation, in contrast to thermoplastic composites.

1.2 Composite properties

Modulus that is orientation dependent and calculated as a volume fraction weighted mean of the matrix (polymer) and filler (fibre) in series or parallel (Equ. 1, where V = volume fraction, E = modulus, c = composite, f = fibre, m = matrix). An efficiency factor (g) is usually included to account for interfacial interaction and variables such as voids, inefficient dispersion of fibre bundles and variations in fibre alignments, etc (Equ. 2). The modulus can be measured using a universal test instrument in tensile mode (parallel with fibre orientation) that emphasises the properties of the fibres. The modulus measured in shear mode emphasises the matrix-fibre interface, while in flexure mode a combination of matrix and fibre modulus is measured, with the upper bended surface in tension and the lower surface in compression (Fig. 1). The Von Mises stress contour diagram (Fig. 1, lower image) shows a stress maximum at the fixture end and a compressive stress maximum in the lower centre surface. The same beam in three-point bend mode emphasises the stress in the load region with compressive stress concentrated near the upper surface and tensile stress concentrated near the lower surface (Fig. 2). An important observation for composite design is that the centre of the beam cross-section is relatively stress free.

$$E_c = V_f E_f + V_m E_m = V_f E_f + (1 - V_f) E_m \tag{1}$$

$$E_c = g V_f E_f + V_m E_m = g V_f E_f + (1 - V_f) E_m \tag{2}$$

Where V_f can be calculated from the length (l) and diameter (d) of fibres and their logitudinal (L) and lateral (S) spacing in the composite.

$$V_f = \frac{\pi l d^2}{4 L S^2} \tag{3}$$

The Halpin, Tsai and, Kardos composite model (Equ. 4 and Equ. 5) is a refinement that contains a geometric fitting parameter, A, where A = 2(l/d) for tensile configuration with E as the tensile modulus, and the aspect ratio (l/d) of length (l) and diameter (d). A numerical solution is obtained for Equ. 4 and Equ. 5 to model a composite modulus.

$$E_c = \frac{E_m(1 + ABV_f}{1 - BV_f} \tag{4}$$

Where:

$$B = \frac{\frac{E_f}{E_m} - 1}{\frac{E_f}{E_m} + A} \tag{5}$$

Fibre composites do not display a yield strength, unlike the matrix thermoplastic, since fibre pull-out and fibre fracture occur intermittently until fracture. Progressive fragmentation of a composite is not well simulated by FEA since the composite structure must be changing to represent structural rupture. Simulation of modulus is made while the composite is still coherent. Measurement of composite mechanical properties provides an overall modulus without information on the contribution of components and variables within the structure. Three assumptions are made: (a). The fibre-matrix interface has perfect adhesion; (b). The fibre and matrix exhibit an elastic response to stress; (c). No axial load is transmitted through fibre ends.

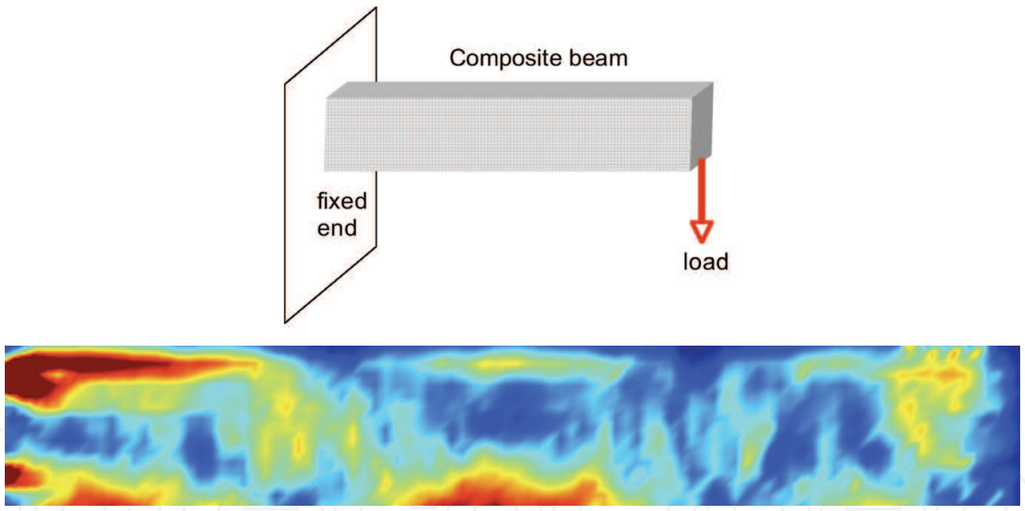

Fig. 1. Supported composite beam with deforming end load (upper) and a Von Mises stress contour plot showing the stress distribution (lower).

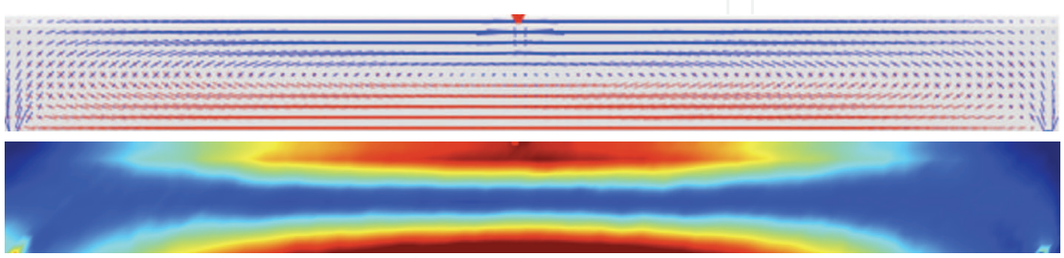

Fig. 2. Beam under three-point bend stress showing compressive stress near upper surface and compressive stress near lower surface, stress distribution (upper image) and Von Mises stress contours (lower image).

FEA requires a proposed model of the composite including the location of fibres within the matrix. The model can be validated by comparison with cross-sectional observation of the composite using optical or scanning electron microscopy. The model should correspond to the actual composite. Inclusion of interfacial interactions within the model is a hypothesis since the interfacial properties cannot be observed. A third phase of strongly adsorbed and immobilised polymer on the surface of fibres can be included to account for interactions (Fig. 3, upper image). The modulus and volume or thickness of this interphase must be estimated as between that of the matrix and fibres. The interphase will be diffused into the continuum matrix. A gradient of modulus can be used instead of a discrete interphase (Chen & Liu, 2001). The nature of the gradient could be linear or non-linear (such as exponential) from the fibre modulus to the matrix modulus. Complex geometry models can be formulated to include various specimen shapes, fibre orientations, woven bundles, and even random voids. The complexity of the model will determine the lowest scale that can be analysed while being representative of the whole composite (Vozkova, 2009). An example of a composite with an enlarged interphase is shown in Fig. 3 (lower image), where the simulation was an application of three-point bend stress. Complex stress fields are associated with the dispersed phase. This type of model is best studied by choice of a single particle or fibre when stresses associated with the interphase are to be considered (see later examples). The concept has been applied to the visco-plastic matrix behaviour of metal composites that reveal similar mechanics to polymer based composites (Shati, Esat, Bahai, 2001).

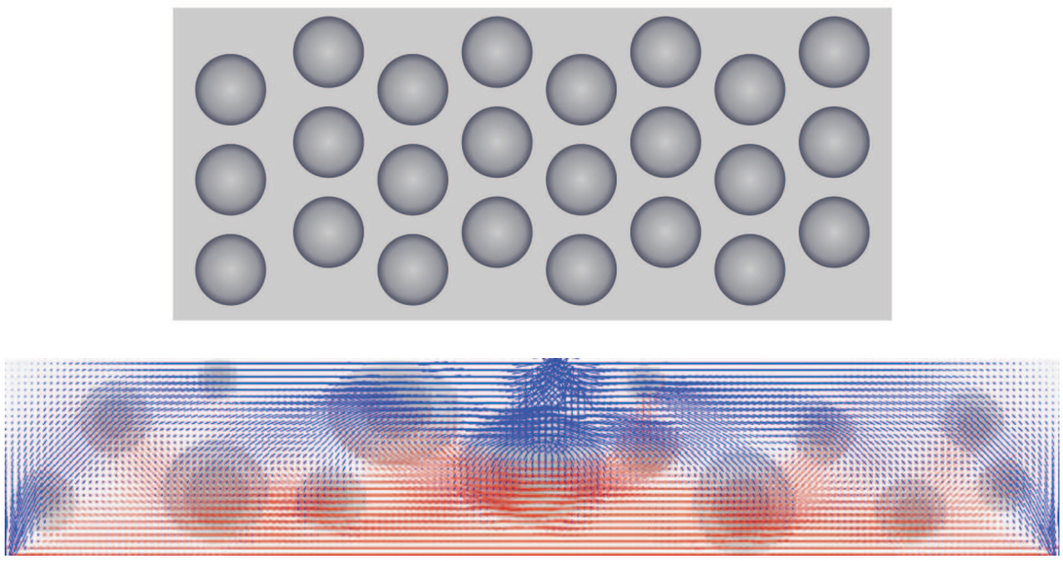

Fig. 3. Fibre composite cross-section schematic showing interphase (darkened) around each fibre (upper) and the lower image shows stress distribution in similar model under three-point bend stress.

The model is then tested by performing a simulation, that is disturbing the model with stress and monitoring the evolution of the strain over time, or applying a strain and monitoring the stress over time. The evolution of the model with time is computed at each node of the finite elements. Application of stress or strain requires that part of the model be fixed. Typically for a beam one end will be fixed and the external stress or strain applied at the other end, for tensile or flexural

(single cantilever bend) testing. Alternatively two ends can be fixed and the stress or strain applied in the centre, equivalent to a dual-cantilever bend. A three-point or four-point bend requires that the ends allow lateral movement or slippage, which is more complex to simulate in comparison to a real situation.
The hypothesis is that the model will behave the same as the real composite. If the hypothesis is correct then the behaviour of the composite will be well understood. If the hypothesis is incorrect them the model needs to be refined and further simulated until the data for the model and real composite converge. Refinement of the model may require inclusion of more variables to better represent the real situation. Unlike a model the real composite is likely to deviate from an ideal structure. Imperfections can be included as discrete entities such as voids, or as a general decrease in the model parameters analogous to an efficiency factor.
An analogy to an anisotropic long fibre composite is reflected in the model of a group of storage silos. Clusters of circular cylindrical structures are found in silos, chimneys and water towers. They are subjected to flexural stress by wind induced oscillations. The cylinders deform in similar fashion to a continuous fibre composite. Five rows of eight silos were modelled using ANSYS with the modulus, Poisson ratio and density as inputs using a harmonic two-node element. The model was validated from data measured in a high wind from ten accelerometers attached to the silo walls. The data revealed harmonic frequencies of the silos relative to the wind velocity (Dooms et al, 2006). The model is structurally similar to a polymer–fibre composite that can display a dimension dependent resonant frequency under modulated force mechanical testing.

1.3 Composite morphological structures investigated using FEA

Important considerations for the design of composites that are assessed using FEA are: The bulk mechanical properties of the composite are determined by the modulus of each phase and their respective volume fractions. Consolidation of the composite is complete and the composite density is a volume fraction average of the component densities. Where consolidation is incomplete this can be represented by a density gradient across the thickness of the composite sheet. Fibre concentration and fibre diameter determine the distribution of fibres since a fixed volume fraction of fibres may be due to few of large diameter or many with small diameter, with a varying total fibre-matrix surface area. The fibre–matrix interface may be implicitly defined such that dewetting or voiding can occur, or be omitted so that the interface will remain intact. Fibre orientation can be included in the model but this will require a larger mesh size to generate sufficient distribution. Fibres are generally included in parallel orientation in models constructed since a random distribution is difficult to model unless the model is large (Fig. 4). The surface versus bulk properties often vary in composites: there may be matrix rich or fibre rich surfaces, with density gradients from the surface to the bulk

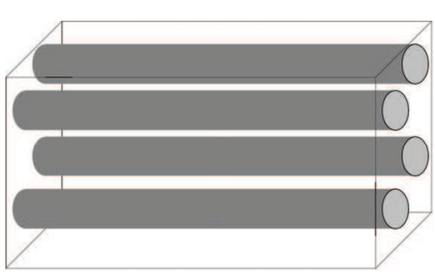

Fig. 4. 3D model of a oriented long fibre composite

A 2D model similar to the fibre composite of Fig. 4 is shown in Fig. 5. The fibres are shown from an aligned view so in the 2D perspective they could be particles. Other similar composite models are shown later in this chapter where the fibres are aligned with the longitudinal axis of the beam. This view of fibre ends is best for observing the stress field throughout the composite and because stress transfer between matrix is better tested laterally for long fibres. In this case the stress is in three-point bend configuration pulling downwards from the right side, while the left side is fixed. The lower section of the beam is in compression, while the upper section is in tension. Some stress concentrations are visible between fibre ends. The regions of stress concentration are between fibres rather than in surface regions; compare Fig. 5 with included fibres with Figs 1 and 2 without fibres, where the stress concentrations emanate from along the surfaces. Stress concentrations between the fibres mean that fracture is likely to initiate at fibre–matrix surfaces or within the matrix between fibres. Strong interfacial bonding and a strengthened interphase will contribute most to a composite in this circumstance. The maximum stress concentrations, both tensile and compressive are associated with the fixed end of the beam, away from the location of application of the stress. Stresses in the compression zone along the lower part of the beam have concentrated where fibres ends are juxta positioned downwards to the left, even though the model was constructed with the aim of randomising the fibre–end positions and diameters. The Von Mises stress plot is not shown because the colour shading obscured the circular fibres end.

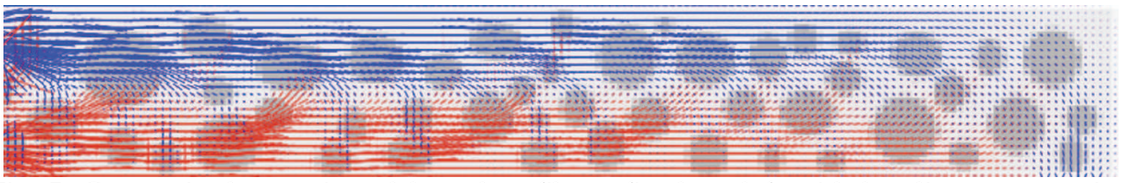

Fig. 5. Composite beam viewed lateral to fibres, fixed on left with bending stress acting down from the right.

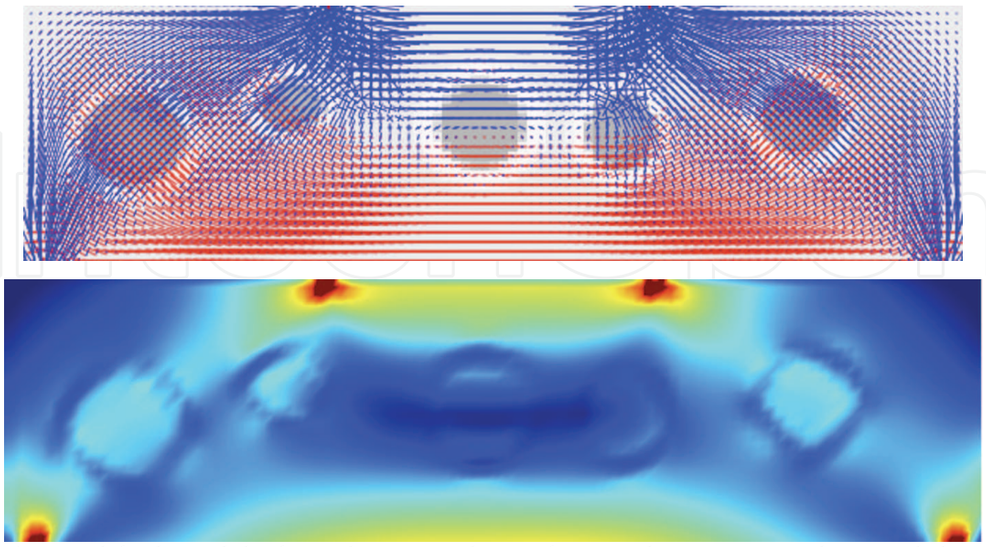

Fig. 6. A simplified model of a polymer with a soft interphase surrounding each hard fibre or particle under four-point stress, stress distribution diagram (upper) and Von Mises contour plot (lower).

A simplified model based on Fig. 5, with fewer hard inclusions surrounded by soft interphase, is shown in Fig. 6. The upper stress distribution diagram shows the compressive stresses passing from the application point through to the supported lower ends. The stress is not concentrated in the vicinity of the fibres, where the lighter shaded areas around each fibre is the soft phase. The lower central section of the beam is under a tensile stress situation. The lower Von Mises contour plot shows the stress reduced zones as darker areas around each fibre. A central stress free zones results from the four-point bend mode radiating stress away from the centre of the beam. Fig. 7 shows the same model as Fig. 6 with both ends fixed to represent a dual cantilever beam instead of a four-point bend configuration. The stress distribution in Fig. 7 is similar though less intense than that of Fig. 6 because some of the stress is redistributed as tensile stress emanating from the top corner fixtures. FEA depends upon the construction of a model to represent a material, such as a composite, and configuring the forces and constraints to best represent either a use situation or to reveal critical zones that are likely to cause performance problems.

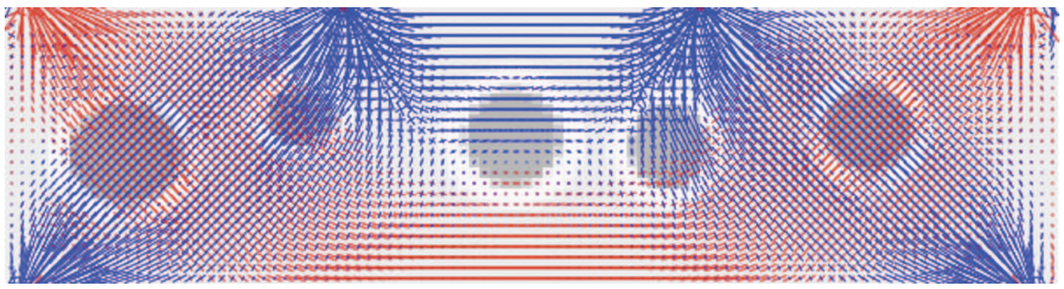

Fig. 7. A four-point stressed dual cantilever simulation of a polymer with a soft interphase surrounding each hard fibre or particle shown as a stress distribution diagram

The contribution of an interphase has been evaluated using a variant of FEA called the advanced boundary element method to model fibre-reinforced composites with consideration of varying thickness boundary layers (Chen and Liu, 2001). Fisher and Brinson (Fisher and Brinson, 2001) have used the Mori-Tanaka model and its extension by Benveniste to study a three-phase composite with either separately dispersed fibre and soft interphase material, that may include voids, or where the fibres were enveloped by the soft interphase material. The Mori-Tanaka model was more effective in predicting the matrix-dominated moduli of the composite. Physical aging was studied by using time and frequency shift factors for these thermorheologically complex materials, with frequency data being preferred. The 2D FEA results demonstrated the importance of the interphase in determining the overall shift rates of the composite. FEA was performed in 2D using a hexagonal array of inclusions with transverse hydrostatic and transverse shear superposition, to obtain the transverse Young's modulus and transverse shear complex moduli.

A composite interphase model was constructed including glass beads, an interphase and polycarbonate matrix, with perfect bonding at each interface and the beads symmetry packed in a cubic array. The Young modulus, stress concentration and stress distribution were simulated. The interphase increased fracture toughness at the expense of elastic modulus, with these observations becoming larger with increase in interphase thickness. A

suitable selection of filler content, interphase stiffness, thickness and Poisson ratio can reduce stress concentration with retention of composite modulus (Tsui et al, 2001).
Stress has been imparted in two orthogonal directions simultaneously on a cruciform shaped specimen (Lamkanfi et al, 2010). The cruciform is applicable to real systems such as rotor blades. Strain was concentrated in the conjunction of the two stresses and concentrated in the corners rather than the centroid of the specimen. The numerical model was validated by experiments by means of a digital image correlation technique. Two- and three-dimensional models were evaluated. An orthogonally stressed cruciform has been simulated independently (Fig. 8) with a fixed point at the centre. The stress distribution (Fig. 8, upper) shows the stresses concentrated in the central region near the corner. This is better depicted in the Von Mises contour plot where the darker shading passes from the arms around the centroid.

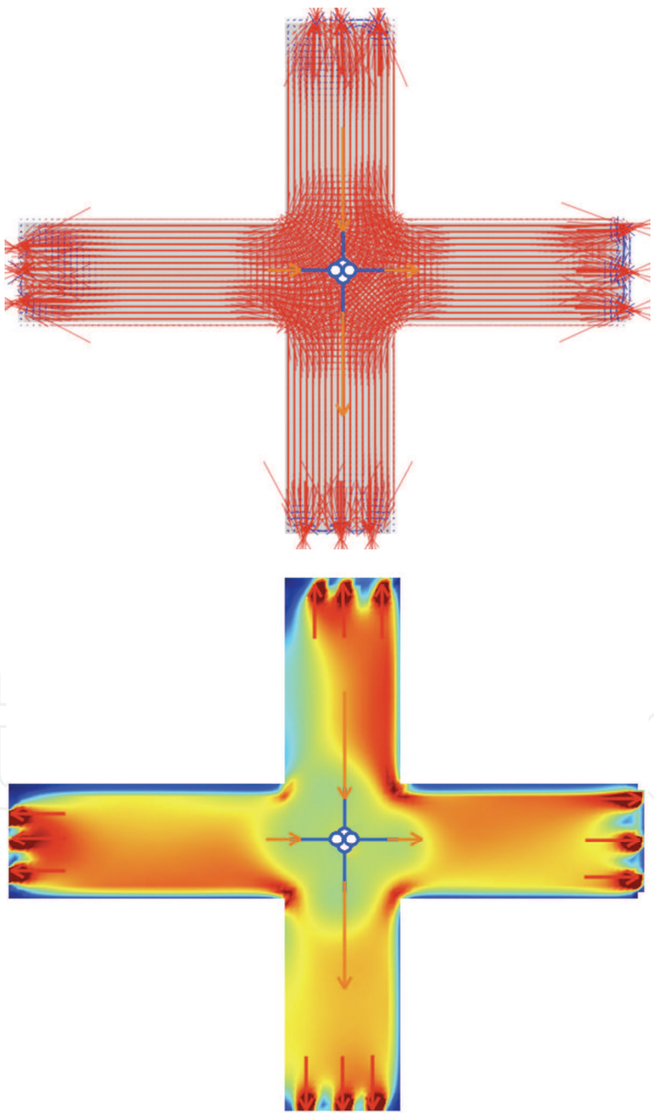

Fig. 8. Cruciform with orthogonal stress, stress distribution (upper), Von Mises contour (lower).

The planar shear bond test has been modelled with consideration of the moduli, bond layer thickness and loading conditions (Dehoff et al, 1995). The model consisted of cylindrical specimens bonded together, and asymmetric elements were used with harmonic stress. Large stress concentrations were confirmed at the bonded interface. The study is directed to assessing whether the shear bond test is useful for understanding the stress states that cause failure and if these stress states exist in clinical dental situations.

2. Computational methods

The finite element method (FEM) is used to solve partial differential equations using approximations that are iterated towards an optimised solution by numerical integration. The process of using FEM to solve practical problems is called FEA. Dedicated software provide the elements for most FEA computations. Examples shown in this chapter were prepared using the ForcePad (version 2.4.2, Division of Structural Mechanics, Lund University, Sweden) two-dimensional FEA program. ForcePad consists of three modes: a sketch mode where the model is prepared, a physics mode where forces and constraints are defined, and an action mode where the FEA calculations are made and the results visualised. The calculations shown in this chapter were performed with a mesh step setting of 6 (fine), vector constraint stiffness scale and force magnitude of 1-10 kN, weight of 1 kN, hard phase elastic modulus of 2 GN, stiffness scale factor of 1000, Young's modulus of 0.35 GN, relative thickness 0.1 and an element threshold of 0.02. Some of the pixelation in figures in this chapter arise from the mesh size used and not the resolution of the images. FEA software often consists of two components, model preparation, such as FEMAP, and the computational engine, such as Nastran.

Commercial software provides a visual and computational environment for application of FEA to problems ranging from simple components to complete complex systems. Typical commercial FEA software are: FEMAP and Nastran, Abaqus, ACTRAN, ANSYS, AcuSolve, ADINA, SLFFEA, LISA, ALGOR, Strand7, AutoFEA, LUSAS, MIDAS, FEAP, JANFEA, CADRE, FEMM, FesaWin, CALCULIX, COMSOL, Visual FEA, FEM-Design, DUNE, FEBio, ForcePAD, JFEM, OOFEM, TOCHNOG, MARC, OpenFEM, SJ MEPLA, FEAMAC, Opera 2D/3D, and many more specialised adaptions of the FEM. Some of the software rely on optional modules for particular and specialised applications. Details of the development and capability of each software package is available from suppliers and any comparison or discussion of performance is a personal choice and beyond the scope of this chapter.

General purpose software such as Mathematica, Matlab, MathCad, Igor, Maple can perform the necessary functions, and some ancillary plug-in programs are available to extend the basic programs. Users design modelling and computational applications within the environment of the software package with the aid of pre-written tools. Many custom written programs are used as described in the literature, which are written from basic principles using languages such as C^{++} and higher level object tools.

FEA experimental design: Description of the actual material, design of the model, validation of the model preliminary calculations, evolution of the simulation with stress, strain and time, analysis of the data. That is the response of each element to the displacement field associated with the environment of the material. Design of the model: finite element or mesh density and pattern, geometry of modelled composite: selected shape and region or finished article, geometry for application of stress or strain, parameters to be modelled (Fig. 9).

Boundary conditions need to be defined together with anchor or fixture points or surfaces. An element mesh needs to be designed and this mesh established a set of nodes in two-dimensions or three-dimensions. The elements can be triangular, tetrahedral, pyramidal, quadrilateral, hexahedral or other depending on the model and the type of problem. Choice of mesh resolution and geometry is important for each model and most advanced software packages provide a range of options and assistance to the modeller to capture smoothness, computational quality, simulation time, curvature and proximity features. Elastic and visco-plastic properties must be defined for the components. The links between elements are the mathematical expressions and their implementation that describe the theoretical aspects of the problem. The component material assembly can be designed as isotropic, orthotropic, anisotropic or laminate structure. The elements can be linear, such as spring, cable, truss, bar or beam. Surface elements include plane, plate, shear or membrane. Solid elements comprise various shapes that may be pre-stressed or face-stressed. The individual elements are allocated structural stiffness, that is a modulus. The modulus matrix is inverted and multiplied with the stress vector to simulate displacement vectors. Recent software includes wizards to assist the analyst in each step of the FEA process.: model design, validation, optimisation and simulation.

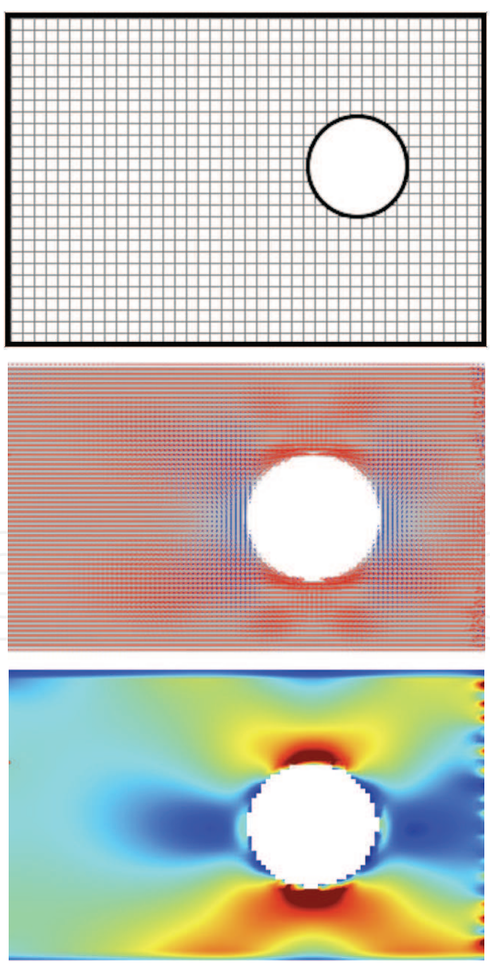

Fig. 9. FEM 2D model of a plaque with a hole for tensile or compression stressing

Validation of the model: Confirmation that the proposed model does portray reality. The model defined in this research used a 3D array of parallel fibres surrounded by matrix. The model did not consider looped entanglements of fibres, though the tensile strength in such cases must be equal to that of a fibre since a fibre must break to allow the matrix to extend. Inefficient wetting and voids are present in real composites, however they are not included in the models because the concentration, shape or distribution of voids is not known. Discrete voids can be replaced by a density gradient in composites that were partially consolidated.
Evolution of the simulation: Input of the material parameters. Digital incrementing of the independent variables. Computation of the dependent variables for each node, within each element, at each increment of stress or strain. The geometry of fixing the position of part/parts of the composite and the location of the displacement field are significant for the evolution of the model.
Analysis of the data. Stress-strain-time curves, analyses of variables between nodes, analysis of variables between composite models. Comparison with continuum composite models.

3. Examples of specific FEA composite simulations

3.1 Laminated composite structures

Damping of laminated carbon and glass fibre plastics is measured as the ratio of energy dissipated to the maximum strain energy stored per strain cycle. A finite damped element model including transverse shear has been used to measure and predict specific damping properties, mode shapes and natural frequencies of the composites (Lin et al, 1984).
Analysis of laminated composites has been performed where the failure mode was delamination of the layers. When a weaker ply fails first, stress will be distributed to the remaining plies and the process will continue giving a progressive failure of the laminate. The modulus of the layers was anisotropic so the strength of the composite depended on the relative orientation of each layer within the overall laminate. Symmetric and anti-symmetric ply laminates with different numbers of layers were formed (Pal & Ray, 2002).
Mechanical properties of a composite depends upon the geometry and aspect ratio of the fibres, while woven fibre composites are distinct from typical unidirectional long fibre composites. A woven fibre composite is usually prepared from multiple layers where the overall composite properties are the sum of the contribution layers. Flexural behaviour is a suitable way to characterise woven or unidirectional composites, since tensile force will be resisted by the modulus of only the continuous fibres. The layers of a woven composite can be divided into unit cells that are the smallest area in which the weave pattern is repeated (Fig. 10). A composite model can be formed by adding units cells laterally and in the thickness direction to form a structure as required for the model. This can be computationally performed by setting periodic boundary conditions. Computations for the property simulation used Abaqus. The FE model used curve beam elements to model warp and weft yarns of the unit cell. This simplified the model yet captured the actual morphology of the woven fibre composite, and hence allowed prediction of flexural modulus. Other weave types and replicating structures are suited to this efficient unit cell model with periodic boundary conditions (Soykasap, 2010).

A model of membrane layers of a laminated fibrous composite (analogous to Fig. 11) addressed the particular issue of interlaminar shear stresses concentrating along an edge region.

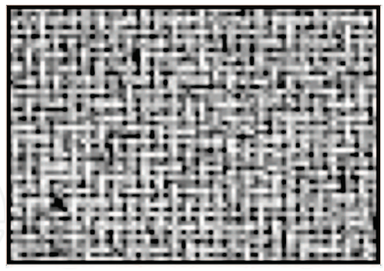

Fig. 10. Standard cross-ply woven fibre mat

The FEA simulation was limited to plane stress, where bending and warping of the laminate have not been considered. The simulated data were favourably compared with corresponding analytical data, with the FE technique presented capable of application in a range of laminate situations involving interlaminar shear stress (Isakson & Levy, 1971).
Through-width delamination of a laminate composite under a buckling compressive stress has been treated using a FEA parametric model. The stress leads to an instability related delamination. Comparison with measured lateral deflections showed that the analysis reflected actual specimen behaviour. Stress transfer was complex and not a simple function of applied stress or lateral deflection, with steep stress gradients at the delamination front suggesting a stress singularity. Hence strain energy release rates were much less responsive than the calculated stresses to mesh refinement. Correlation of the calculated strain energy release rates for mode I and II crack extension with actual delamination growth rates showed that delamination growth was dominated by mode I, even though mode II strain release rate was numerically larger (Whitcomb, 1981).

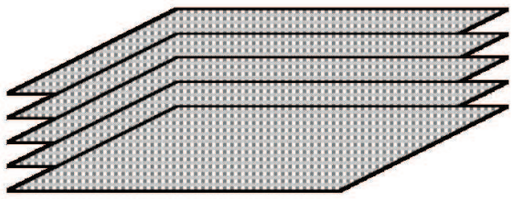

Fig. 11. A multi-layer woven fibre laminate composite

Orthogonal woven composites were studied using a 3D unit cell model using a custom approach followed by Strand6 FEA software. The woven fibre composite was for aerospace application, typically an epoxy-graphite fibre structure. The structural variables included geometric parameters, yarn volume fractions and engineering elastic constants. The in-plane modulus predicted using the unit cell model and a laminate model corresponded with experimental data form the literature (Tan, et al, 1998). Two-dimensional models were presented for the elastic analysis of a plain weave glass or carbon fabric epoxy resin laminate, with the aim of developing a simple though generalised model that will enable interpretation of the two-dimensional extent of the fabric, and the contribution of various fabric geometry parameters. This was intended for prediction of in-plane elastic modulus and selection of fabric geometry for any specific application. The fibre volume fraction

depended on weave geometry for a constant global fibre volume fraction. The elastic modulus predicted increased with fibre undulation, but reduced for 2D prediction and remained constant for a 1D parallel model with lamina thickness increase (Naik & Shembekar, 1992).

An example of a 2D to 3D global/local FEA of a laminated composite plate with a hole is presented. 2D models have shown limitations that can be addressed by using 3D models, though in many cases a 3D model is computationally inefficient for a particular task. An alternative is to perform a detailed 3D analysis on a local region of interest, followed by a more extensive, in geometry, stresses or time, simulation using a 2D model. In the example presented the local region of interest is the hole, around which the interlaminar stresses need to be examined in detail. There appeared to be a critical hole size in the laminate where the interlaminar stresses were maximised. A reduction in hole size for 3D laminates under compression suggested that if the hole contained a fastener, failure could result as the laminate fibres would be crushed into the rigid fastener. The degree of thickening of laminates under compression, around the hole, varied with lay-up, hole size and position about the hole (Muheim & Griffen, 1990).

Progressive failure of plain weave composites subjected to in-plane extension has been simulated using 3D FEA. Stress was parallel to the tow orientation and tow waviness was considered. The predicted strength decreased with tow waviness as progressive delamination occurred (Hyung, et al, 1991). The fibre shaping process in textile composites was evaluated from biaxial tests on cross shaped specimens. The influence of undulation variations in the weave and of interactions between the warp and weft were variables considered. The total energy was calculated as the sum of energies of each elementary cell that can repeat to form the entire composite. The weave undulations and interactions contributed to decline of the mechanical behaviour of the fabric composites (Boisse, et al, 1997).

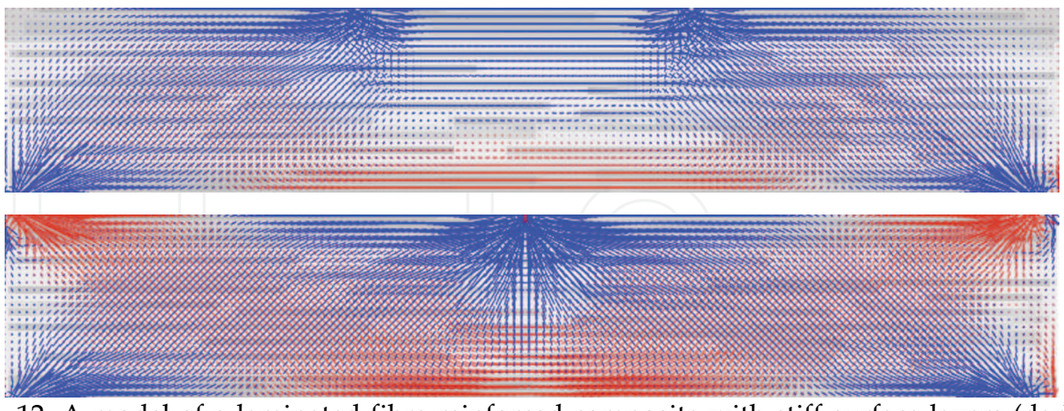

Fig. 12. A model of a laminated fibre-reinforced composite with stiff surface layers (darker shading) and a central softer layer under four-point bend (upper) and three-point dual cantilever (lower).

The laminated composite model shown in Fig. 12 has stiffer surface layer where resistance to stress is most important and a softer central layer where stresses from deformation modes is least. In practice the central layer could be a foam or material with limited consolidation. Each of the layers is reinforced with the same type of fibres. The simulated was performed

under four-point bending (upper image). A compressive stress concentration radiates from the application points to the two supported lower corners. A tensile stress is situated along the higher stiffness layer at the bottom. Stress transfer to fibres is visible throughout the laminated composite, but mainly as expected from regions of higher stress. A three-point dual cantilever simulation of the laminated composite is shown in Fig. 12 (lower). The stress concentrations are more intense with tensile stress regions emanating from the upper corner fixtures and and in two localised regions along the bottom layer. Stresses are greater in the stiffer matrix top and bottom layers and stresses are transferred to fibres throughout, though with increased intensity in the higher stress regions of the upper and lower layers of the laminate.

3.2 Anisotropy of thermoplastic composites

Orientations occur during processing operations such as extrusion and injection moulding. Fibrous and platelet fillers are orientated along the extrusion direction or along the more complex flow lines in injection moulds. This directional geometry of the fibres is normally welcome as maximum modulus and strength are required in the machine direction. These orientations simplify the preparation of finite element models and the simulation process. An anisotropic fibre composite is shown in Fig. 13 (left) with the stress applied parallel to the fibres. The stress concentrations are low and concentration in regions where the fibres were made shorter. When the stress was applied transverse to the fibres (right) the stress concentrations were much greater throughout since the lower modulus matrix carried more of the stress than the higher modulus fibres.

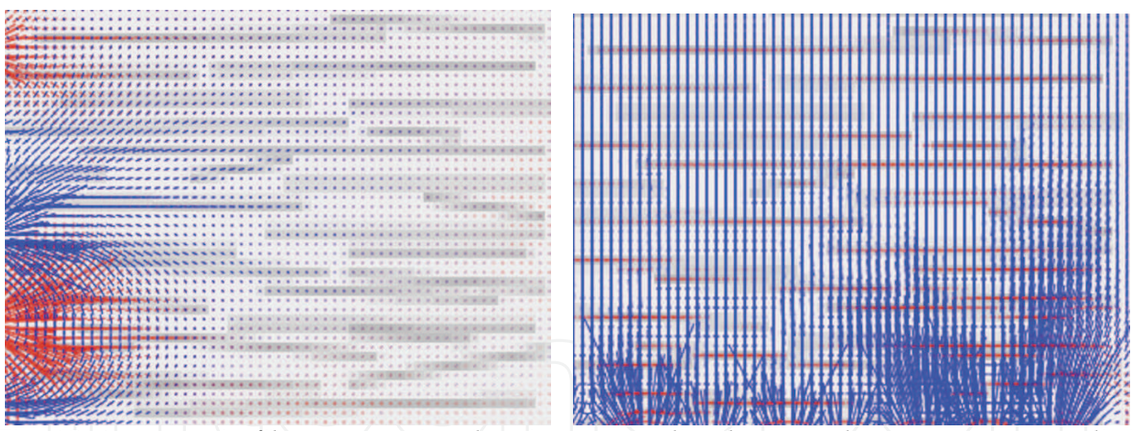

Fig. 13 Anisotropic fibre composite showing stress distribution when stress was applied parallel to the fibres (left) and transverse to the fibres (right).

A more complex consideration is anisotropy of the molecular or supramolecular structure within the matrix. Shear flow causes preferential orientation of molecules, crystallites and crystallite assemblies along the flow contours. Thus a polymer matrix will posses anisotropy of properties such as modulus, Poisson ratio, density fluctuations, residual stress, strength and ultimate properties such as toughness, break stress and strain. The anisotropy arising from these molecular considerations is difficult to accommodate in a model and subsequent simulation of the application of stress or strain. They are difficult to consider when interpreting actual performance properties of polymer composites since any detailed

molecular structure or morphological structure is difficult to measure and usually unknown to the tester and materials designer. The microstructure of the composite is known to be the determinant factor for the properties of fibre reinforced composites (Maligno, Warrior, Long, 2008).

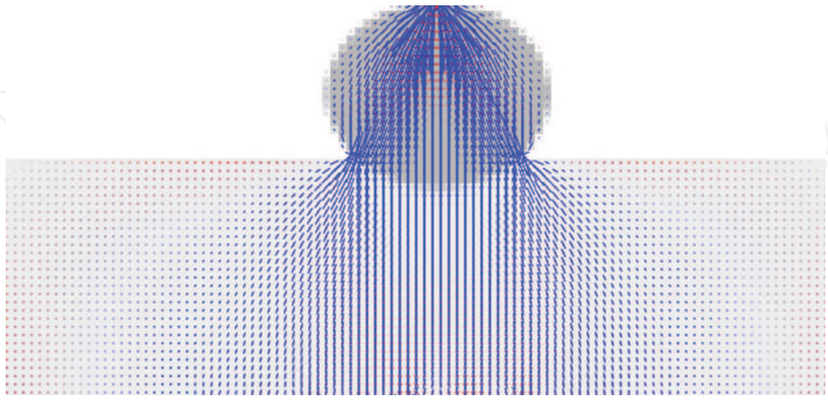

Fig. 14. Stress distribution diagram for indentation of a soft material by a hard round object.

A three-dimensional finite element model was used to evaluate indentation of polypropylene–cellulose fibre composite to determine the elastic modulus and hardness. FEA was conducted using a rigid flat cylindrical disk with a radius of 1 μm with Abaqus. Indentation to 50 or 100 μm depth provided no difference in the unloading values. Analysis of the interphase region showed a 1 μm wide property transition zone, though this zone could not be isolated from the contributions of the adjacent polypropylene and cellulose fibre properties (Lee, et al, 2007). An analogous model is shown in Fig. 14 in 2D and the simulation was performed with stress applied to the hard round object while the soft material was supported along its base. The stress diffuses from the application point with concentrations at the edge where the round object meets the soft material. Indentation by such a blunt object is not as critical as when a crack has been induced and the crack tip provides a focal point for stress concentration.

3.3 Composites with the same material for fibre and matrix

All-polypropylene composites have been prepared from polypropylene fibres with a lower melting temperature polypropylene matrix that may consist of a random polypropylene copolymer, different polypropylene tacticity or a different crystalline allotrope of polypropylene. The different melting temperatures of the polypropylene fibres and matrix are required so that the matrix can melt and form a continuous phase around the fibres without changing the oriented crystalline morphology of the fibres (Houshyar & Shanks, 2003). All-polypropylene composites can be prepared from polypropylene film-fibre layers, felted interwoven fibres of different melting polypropylenes, fibres impregnated with lower melting temperature polypropylene powder, fibres impregnated with polypropylene solution (Houshyar et al, 2005). Adhesion between polypropylene matrix and polypropylene fibres was characterized using a micro-bond test inspired by a fibre pull-out technique. The results showed that adhesion was appreciably increased when polypropylene fibres were used instead of glass fibres in the matrix (Houshyar & Shanks, 2010).

Finite element analysis showed that fibre volume fraction and diameter controlled stress distribution in all-polypropylene composites. The stress concentration at the fibre-matrix interface was greater with decreased fibre volume fraction. Changes in fibre composition were present in high stress regions. Stress concentration at fibres decreased and interfacial shear stress were more severe when higher modulus fibres were included. The relation between matrix and fibre modulus was significant, along with the interfacial stress in decreasing premature interfacial failure and enhancing mechanical properties. The simulations revealed that low fibre volume fraction provided insufficient fibres to disperse the applied stress. Under such conditions the matrix yielded when the applied stress reached the matrix yield stress, resulting in increased fibre orthotropic stress. With high fibre volume fraction there was matrix depletion and stress transfer had diminished capacity (Houshyar et al, 2009).

3.4 Biomaterial composites

A compromise in the design of biomaterials is the need for soft tissue bonding materials in contrast to hard wear resistant materials particularly in restorative dental composites. An approach is to use low modulus adhesive linings to release stress due to contraction during cure. Alternatively polymer without filler or lightly filled can be used as a low modulus relatively thick bonding layer to reduce the gradient to a high modulus restorative material. The FEA study aimed to predict the adhesive lining thickness and required flexibility. The model used a tooth shape connected by spring elements, constructed with 3D CAD using digitised images of a scaled tooth plaster model, and exported to Pro-Engineer, while FEA used ANSYS. The FEA determined optimum adhesive layer thickness for maximum stress release, though the models showed that a thin flexible adhesive layer had the same efficiency as a thicker higher modulus adhesive layer Ausiello, et al, 2002).

Polymer glass and carbon fibre reinforced dental posts were modelled to compare properties with those of gold alloy cast posts, using a natural tooth restoration as a reference. The models contain continuous, unidirectional fibres that were uniformly packed. The models were formed with reference to the actual geometry of an upper central incisor. The model meshes were created using Mentat software package and they were simulated using MARC solving code. Mechanical data was obtained by three-point bend testing and compared with the FE model results, under various loading conditions. The glass fibre exhibited lowest peak stresses because its modulus was similar to that of dentin, and thus similar to the natural tooth (Pegoretti, et al 2002).

The stress contributions and stress rates within posterior metal-free dental crowns made from new composite materials were investigated. An FEM of a first molar was constructed, and placed under load simulating maximum bite force and mastication force using FEA. The maximum stress concentrated about the loading point. When a load was applied horizontally it was found to be a critical factor determining failure (Nakamura, et al, 2001).

The fatigue and fracture characteristics of human bone subjected to long term dynamic loading may be due to gradual reduction of elastic modulus resulting from various strain environments. The FEM applied to these materials will establish information for the design of joint replacements. Femoral neck fractures were chosen as a situation in which to explore FEA using continuum damage mechanics applied to the fatigue behaviour. Minimal modulus degradation or accumulation of permanent strain was observed until near the end of their fatigue life, and the models were unable to predict the rapid deterioration in the last

stage of this fatigue life. Models subjected to high initial strain, low cycle fatigue showed continuous modulus degradation and permanent strain accumulation throughout the test (Dooms, et al, 2006).
A natural fibre reinforced composite was studied using a shadow moire method to find the whole-field deformation of a cantilever beam under static stress, and the results compared with FEA in the same configuration. The comparison revealed a non-zero stress gradient in the cantilever due to the clamping force (Lim, et al, 2003).

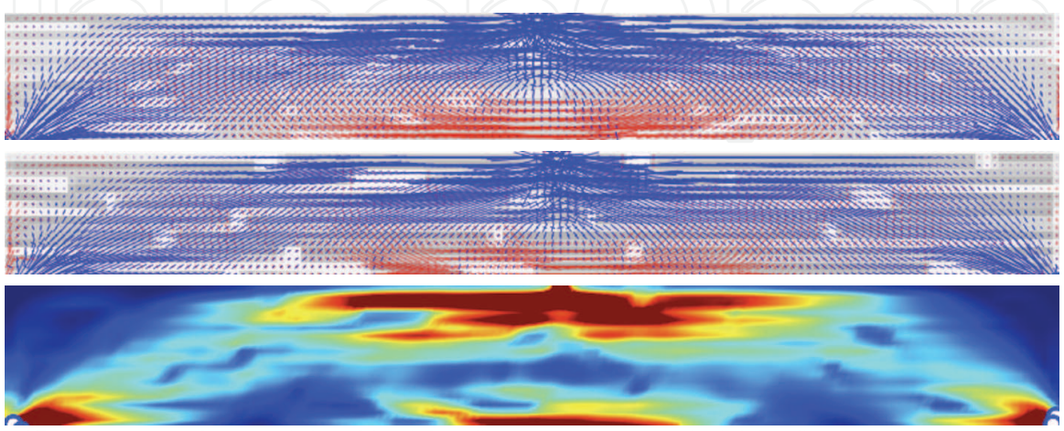

Fig. 15. A composite model with thin fibres (upper) and thick fibres at about the same volume ratio (centre) with Von Mises representation of the thick fibre composite (lower) after three-point bending.

The contribution of thin fibres (3 units) compared with thick fibres (10 units) in a composite with approximately the same volume ratio, is shown in Fig.15. The simulation was in three-point bend configuration with the same stress applied to each composite. Compressive stresses distribute from the upper centre application point to the supports at the bottom ends. The stress intensities are the same with thin and thick fibres. The lower centre region of both composites is under tension and the intensity of stresses appears greater where thin fibres were included. Horizontal streaking of the stresses represents stress transfer to the fibres. The model does not include a interfacial bonding that will be a factor in a real composite. This is probably why there is not a significant distinction between the composite models containing thin or thick fibres. Thin fibres present greater surface to the matrix and will thus provide improved bonding. The thick fibre composite is shown as a Von Mises contour plot (Fig. 15, lower) to emphasise the stress concentrations as mainly near the point of stress application, at the left and right supports and for the tension zone along the lower edge.

3.5 Nanocomposites

Polymer composites with carbon fibre were studied using a homogenisation method that included aspect ratio and concentration of the filler, in a controlled volume finite element method. The composites were assumed to have geometric periodicity at the local length scale and orientation of the carbon nanotubes was considered. The model showed thermal conductivities from numerical prediction were higher and rose more steeply with aspect ratio or volume fraction than those from experiment. Overall the calculated and

experimental values were similar (Sun & Youn, 2006). The mechanical properties of metals discontinuously reinforced with ultra-fine micro-structures have been studied by finite element methods (Huang, Bush, 1997).

Carbon nanotubes (CNT) are finding increasing application in composites because of their high modulus and electrical conduction. Carbon nanotubes are of molecular dimensions and consist of one large molecule so molecular mechanics should be an attractive modelling technique (Fig. 16) Mechanical properties can be better evaluated using FEA. Single-walled (SWCNT) and multi-walled (MWCNT) varieties are available. A CNT is a cylinder of graphitic carbon atoms bonded on the surface in a hexagonal array consistent with a space-frame structure. The hexagonal covalent bonding has been used as beam elements for a mesh for FEA using ANSYS software. The contributions of wall thickness, tube diameter, bonding chirality, on the elastic modulus of SWCNT were investigated. The elastic modulus decreased with wall thickness and increased with tube diameter (Tserpes & Papanikos, 2005). The space-frame model of CNT described merges the real-world scale functions of FEA with those of molecular mechanics at the atomistic scale, equating the modulus of the frame with the force field of the covalent bonds.

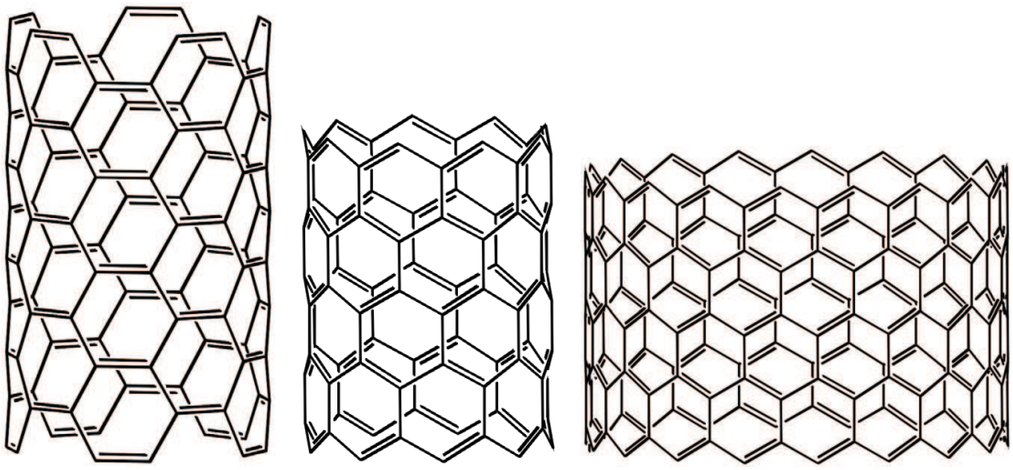

Fig. 16. Carbon nanotube structures, 5,5-armchair (left), 9,0-ZigZag (centre), 18,0-ZigZag (right)

Carbon nanotube reinforced polymers show significant enhancement over the polymer alone with regard to mechanical, electrical and thermal properties. The characteristic waviness of nanotubes embedded in a polymer was investigated in response to impact of their effective stiffness. A 3D FEM of a single infinitely long sinusoidal fibre within an infinite matrix was used to numerically compute a dilute strain concentration tensor. The modulus reduction was dependent on the ratio of sinusoidal wavelength to CNT diameter. As the wavelength ratio increased, the modulus of the composite with randomly oriented wavy CNT converged to that of straight CNT inclusions. The model developed can be used for other CNT-reinforced polymers, including different CNT configurations, viscoelastic response, low matrix-CNT bond strength, thermal and electrical conductivity (Fisher, et al, 2003).

3.6 Composites with particulate filler

A model has been prepared for a glass sphere filled epoxy for comparison with glass fibre fillers in the same polymer. The model considered spheres of equal diameter randomly distributed within an infinite matrix. The section for FEA was a cylinder containing a single sphere at its centre and LUSAS software was used for computations. The FEM was validated by agreement between predictions and experimental measurements that will lead to more efficient use of these materials under varying stress conditions (Guild & Young, 1989). Such a model is illustrated in Fig. 17 (left), while a 2D representation after simulation with compressive stress is shown as a stress distribution (centre) and Von Mises stress contour image (right).

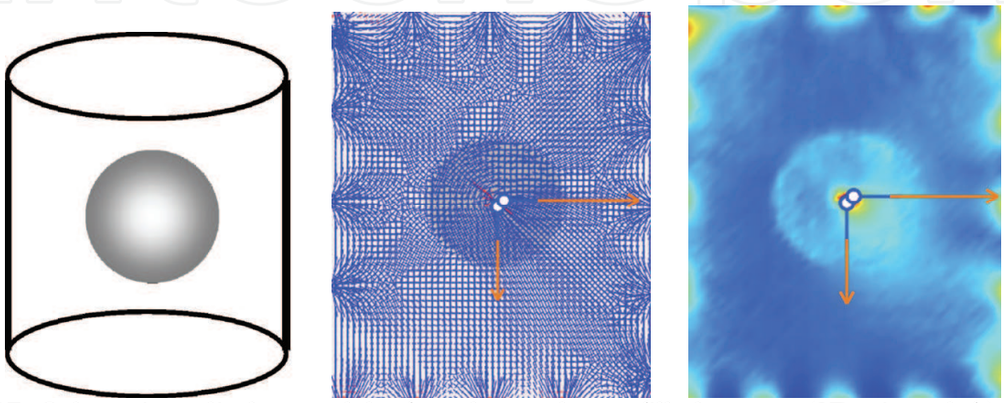

Fig. 17. Sphere in cylinder model of a glass spheres filled epoxy (3D view, left), after simulation under compressive stress showing stress distribution (centre) and Von Mises stress contours (right).

The arrows in Fig. 17 show the anchor points at the centre of the hard particle. An identical Von Mises stress contour plot was obtained when tensile expansive stress was applied.

3.7 Composites containing stress concentrations

Stress concentrations are prevalent in composites due to their formation from two dissimilar materials. Stresses may originate from differential shrinkage during cooling, crystallization of the polymer matrix, solvent evaporation, cure of reactive polymers and viscoelastic memory after polymer matrix flow. During matrix transformations the filler or fibre dispersed phase is typically inert. Stresses in laminates have been analysed by consideration of material non-linearity. Tensile stress was applied in a simulation and damage accumulated was calculated according to a property degradation model, until a failure criteria was reached. The model and simulation data was compared with experimental measurements on laminates containing a circular hole (Chang & Chang, 1987).

A composite design to avoid thermal shock and high strain rates is a functional graded material (FGM). FGM are designed to have a relatively graded variation of structure rather than a sudden change at interfaces that will produce stress concentrations that weaken interfaces. FGM is achieved by the composite preparation technique, such as formation of a continuously varying volume fraction of filler particles in the polymer matrix. FEA analysis of a FGM used Nastran with a plane stress elastostatic model and a symmetric three-point bend test simulation. The mesh discretization used consisted of rectangular eight-node

isoparametric elements. The Young modulus was varied within the model while maintaining a constant Poisson ratio. The FEA fracture analysis demonstrated that the FGM were better than a bimaterial counterpart (Butcher, et al, 1999).
Residual stress concentrations may be due to chemical reaction shrinkage during cure, temperature stress from non-equilibrium cooling particularly past the glass transition temperature, and humidity that will contribute swelling and contraction with variation in water absorption. A method of spring-in, with a right-angle model, was used to identify stress in curved components in composites with woven and chopped fibre reinforcement. The residual stress level in the angled region of the model was calculated and indicated the volume affected by the deviation from structural equilibrium (Wang, et al 2000).
Residual stresses remain in composite as a consequence of thermal relaxation kinetics upon cooling. Stresses are relieved over time by creep and stress relaxation and with annealing temperature treatment to change the thermal history. These considerations applied to many polymer systems, but analogous situations exist within inorganic composites. One study investigated aluminium oxide fibres in a metal alloy matrix of nickel-aluminium. A FEA model was simulated using Abaqus software. The evolution of residual stresses over time was interpreted in response to creep, plastic deformation and cooling/heating rate path dependency (Choo, et al, 2001).

3.8 Fibre-Matrix interfacial adhesion

A rigorous composite model needs to give attention to explicit bonding between the matrix and fillers, which are often fibres, but may be platelets, spheres or irregular particles. Bonded joints provide the connecting system whereby stress is transferred from the relatively low modulus matrix resin to the supporting high modulus fillers. A non-linear model was necessary to achieve accurate results relating a standard adhesion test experimental data with numerical data. Stresses concentrated at the interfaces at the longitudinal and transverse ends of an adhesive layer (Diaz, et al, 2010). Analyses and interpretation of adhesion strength needs to consider the viscoelastic nature of polymers, such that much energy in separating bonded interfaces is expended in the bulk polymer due to viscoelastic processes converting stress energy into heat energy resulting from molecular segmental motion friction. The relationship between stress transfer, the elastic modulus and the mechanical properties depicted by a stress–strain analysis have been simulated by finite element analysis (Kang, Gao, 2002).

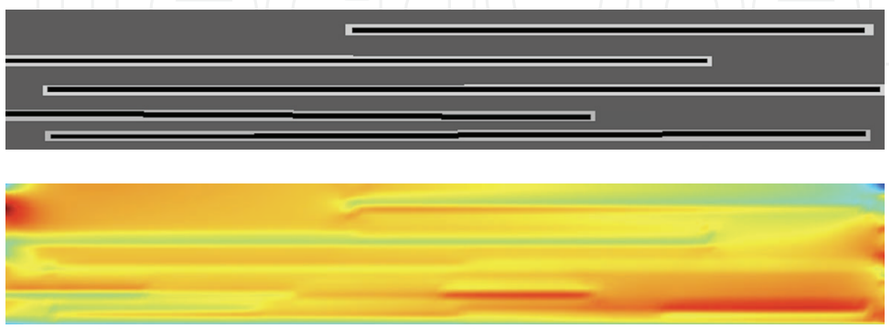

Fig. 18. The model (upper) of composite with fibres with a weak interface, and after simulation showing Von Mises stress (lower).

Fig. 18 shows a representative model of a fibre composite with a weak interface, represented by the lighter shading around each fibre. After simulation of a tensile stress the Von Misses stress distribution shows that stress has not been transferred to the fibres as well as in a composite with a strong fibre-matrix interface (see lower region of Fig. 18).

3.9 Impact initiated delamination

Laminar fibre-matrix composites are subject to failure by delamination under various loading modes and loading rates, including impact forces. The interface strength and deformation behaviour are critical laminate characteristics to be evaluated. Crack growth can be suitably initiated by including interlaminar cracks in the model. Bending, shear and mixed loading modes have been used in the failure simulations. An interface element was use to describe resistance to crack growth (Wisheart & Richardson, 1998).

The resistance to impact has been investigated when composite laminates were subjected to an initial stress. A shear flexible plate composite model was impacted by a mass during the simulation. Finite element analysis was used to solve the contact force and the dynamic response of the composite plate. The initial tensile stress amplified the effect of the impacting mass, while an initial compressive force attenuated the effect of the impacting mass (Sun & Chen, 1985). Barely visible impact damage was predicted using FEM of the larger scale structure. The model included dynamic responses including stress and strain history. The method was validated using experimental data from carbon fibre epoxy composites, and the approach was extended to glass fibre and Kevlar laminates (Davies, et al, 1994).

Low velocity impact damage to composite laminates results in complex cracking of matrix and fibre, and delamination. The complexity of the fractures makes prediction a difficult challenge, since the failure mechanisms are disperse. A FEA of post-impact damage zone with compression buckled delaminated fibres has been undertaken to assess the strength reducing mechanisms. Comparison of the FEM with laminates containing artificially induced damage has demonstrated consistency between prediction and observation (Pavier & Clarke, 1996). Damage mechanisms and mechanics of laminated composites due to low velocity impact has been evaluated (Hyung, et al, 1991).

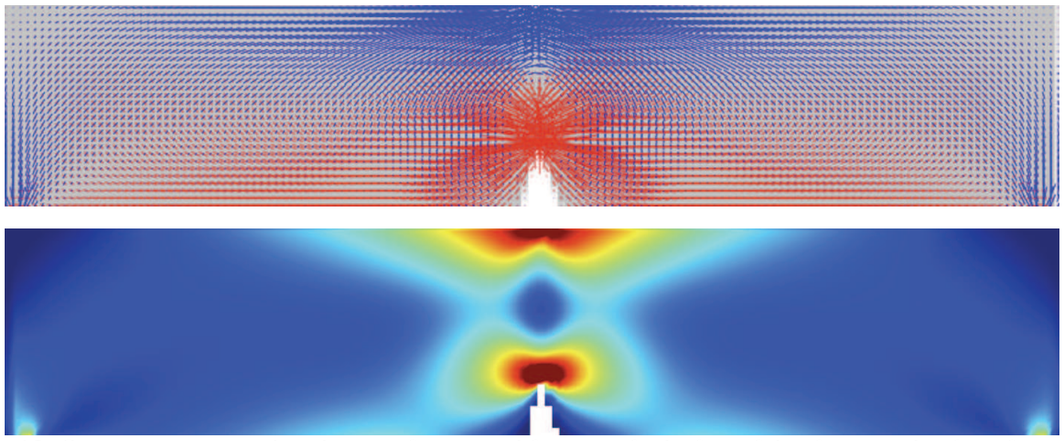

Fig. 19. Stress concentration in a polymer with a crack, induced in three-point bend mode, stress distribution diagram (upper) and Von Mises contour image (lower).

Prediction of damage development to failure in composites is important for assessment of applications. Progressive damage evaluation using FEA can predict potential damage that is often unobserved. 3D FEA of carbon fibre epoxy composites used Abaqus with specially designed meshes to identify criteria to evaluate the onset and reduction in properties due to local damage (Gamble, et al, 1995).

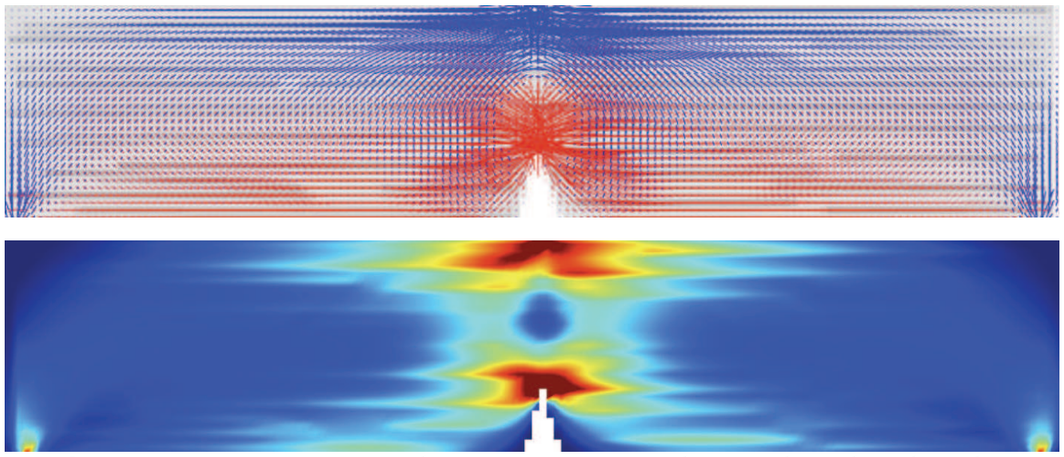

Fig. 20. Stress concentration in a polymer composite with a crack, induced in three-point bend mode, stress distribution diagram (upper) and Von Mises contour image (lower).

Damage development in a polymer is accelerated by the presence of a crack as illustrated in Fig. 19 where application of a stress in three-point bend mode has caused stress tensile concentration at the crack tip and compressive stress concentration at the point of stress application. The stress diagram (Fig. 19, upper) shows the tensile stresses radiating from the crack tip, a situation that is likely to result in crack opening, growth and failure. The Von Mises contour representation (Fig. 19, lower) emphasised the intensity of the stress concentrations. The same FEA simulation of a polymer composite with fibres parallel to the axis of the beam is shown in Fig. 20. The stress concentrations are almost the same as in the plain polymer except that stress has been transferred to the fibres and can be seen to radiate away from the crack tip and application zone along the adjacent fibres. Transfer of stress to the fibres is more clearly seen in the stress distribution diagram (Fig. 20, upper) where the fibres are the darker horizontal lines. The Von Mises contour plot show the stress transfer to fibres are the lighter streaks emanating laterally from the central stress zone.

3.10 Contribution of broken fibre and fibre pullout

Stress concentration at a broken fibre has been simulated by a model including a single broken fibre surrounded by six equally spaced complete fibres in an epoxy resin, based upon a fibre volume fraction of 0.6. The model and separately each component were simulated as a homogeneous, orthotropic material. The stress affected fibre length was half the ineffective broken fibre length (Nedele et al, 1994). The contribution of fibre fracture or a fibre end is typically measured using the single fibre pull-out test. The matrix is fixed in position and a tensile force is applied to the fibre (Wong et al, 2007). A 2D axisymmetric linear finite element model has been developed for fibre pull-out to meet the criteria: energy release rate for interface crack extension, large fibre aspect ratio, singular stress field at the

crack tip, and interface crack initiation for short crack lengths. Interface crack initiation occurred under definite unstable mixed mode conditions, complicating the interpretation of the critical energy release rates (Beckert & Lauke, 1995). A model containing a region of broken fibres is shown in Fig. 21. After simulation under a tensile stress the Von Mises stress contours show that most stress transfer to fibres occurs in the lower region where the fibre ends are overlapped. In the broken fibre (upper) region the stress intensities are low, particularly in the regions between breaks. A consequence is that the broken fibre region is not supporting its share of the stress, and the undamaged region has increased stress concentration that would be likely to cause further fibre breakage in a real situation. Fibre pullout is analogous in that low interfacial bonding will limit the stress that can be transferred to the fibres and the matrix will be more able to deform in the weakly bonded regions.

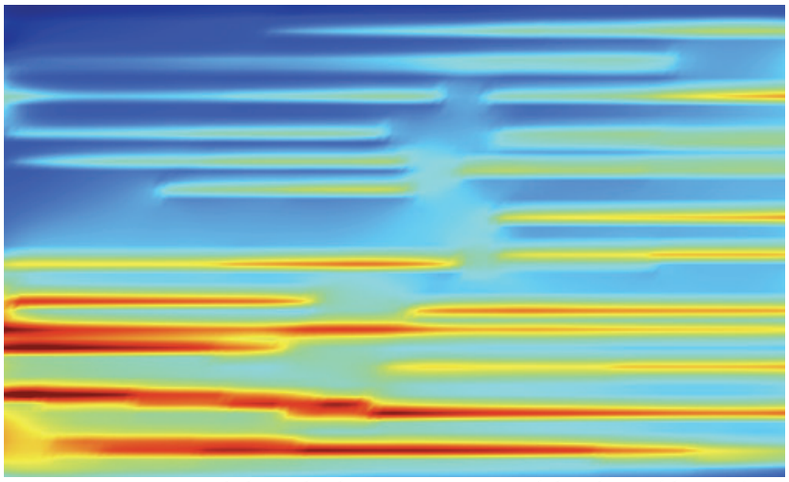

Fig. 21. A fibre composite model including a region of broken fibres (top section) with mostly continuous or overlapping fibre (lower section).

Models for the debonding of a fibre embedded in a brittle matrix have been proposed and assessed. The analysis was in the frictional sliding zone where axial and radial stresses are characterized along the z-axis by a Lame problem that is illustrated in the article. Steady state stress release rate is evaluated in the absence of friction and the upper limit to interface toughness for mode-2 debonding. Some specific cases considered are: debonding with constant friction, debonding with Coulomb friction, and fibre pullout with constant friction. This method was based upon the use of a continuous distribution of dislocations in an integral equation formulation to replicate a crack. The study was confined to materials having a residual compressive stress across the fibre-matrix interface (Hutchinson & Jensen, 1990).

Matrix dominated failure in polymer composites can be modelled by using cohesive zone interface elements. These elements have been shown to enable simulation of actual failure mechanisms that proceed via damage development through to failure. Cohesive zone elements accurately simulate delamination, in-plane failure of laminates, notch sensitivity, impact fractures through to ultimate debonding failure Wisnom, 2010).

3.11 Mechanically fastened composites

Composites gain strength from transfer of stress from matrix to high modulus filler, typically fibres. However composites are often mechanically fastened, which requires disruption of structure by a hole with fastener and stress concentration sites at the points of fastening. Observations of failure modes reveal three types: tension, shear-out and bearing. The stress distribution in the model was determined by a finite element method, then the failure stress and failure mode were predicted from a failure criteria hypothesis. The failure mode for a specified stress has been found to depend upon: material properties, joint geometry and fibre ply orientation (Chang et al, 1982). Three-dimensional models of composites with single- and multi-bolt holes with variation in hole clearance were simulated by finite element analysis of shear. Increasing clearance reduced the stiffness of single-bolt joints and changed the load distribution in multi-bolt joints. The simulation results agreed with experiments demonstrating that the finite elements models can become a routine part of the design process (McCarthy, 2002). Fig. 22 demonstrates a mechanically fastenable plaque with three holes that can be potentially bolt holes. The plaque was simulated under compression and the stress distribution diagram (upper image) shows compressive stress lateral to each bolt hole, with tensile stress along the upper and lower edges of each hole. The Von Mises contour diagram (lower image) shows a high stress intensity along the top and bottom edges of each hole, with localised stress along the line of holes especially between pairs of holes.

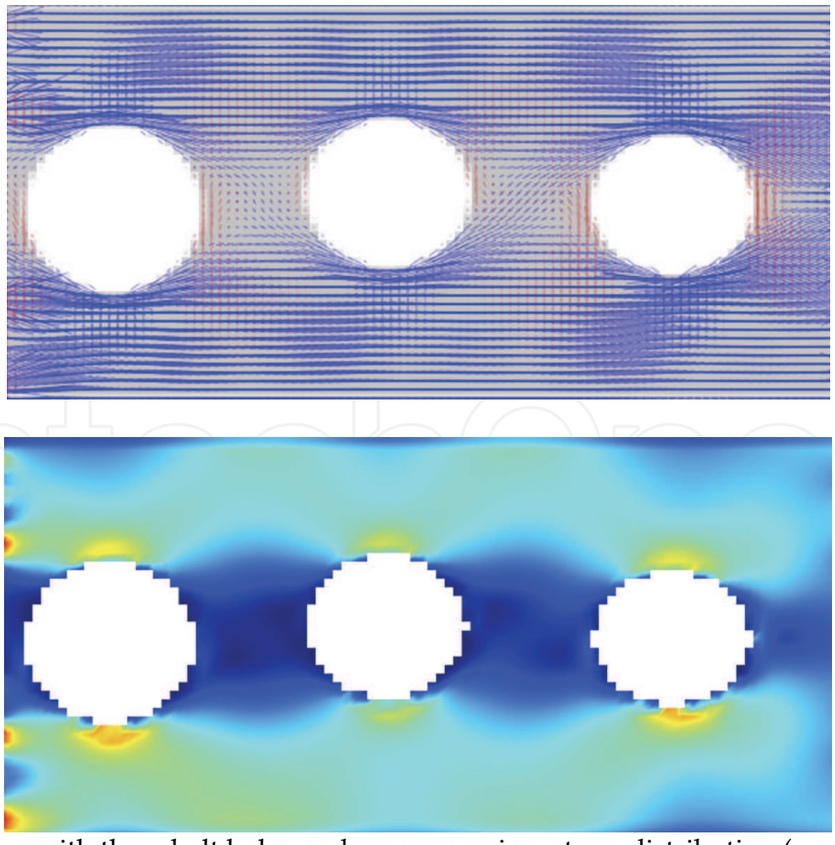

Fig. 22. Plaque with three bolt holes under compression, stress distribution (upper) and Von Mises stress contours (lower).

3.12 Scale and model composite computations

FEA models are mostly of a scale directly relatable to the real system being modelled. The properties of each phase and any discrete interface are global parameters that define the materials and their interactions. The nature of the structure is important for the model to represent the actual composite. However, the components within the composite can be changed by changing the material parameters. For instance, a nylon–glass fibre composite can be changed to a polysulfone–carbon fibre composite by changing the material properties of the respective polymer and fibre, the structure of the composite remains essentially the same. This is because the molecules structure of the polymer and filler is not considered in the model. The same composites could be converted into an epoxy–carbon fibre composite since the model does not differential between a thermoplastic and the highly crosslinked epoxy structure.

A decrease in the scale to micron dimensions brings the model into the realm of meso-materials. At the meso-level discrete atoms are not represented, but molecular are introduced as consisting of beads or chords that are allocated properties consistent with or derived from combinations of real atoms or molecules. Thus the chemical nature of the components of the polymer and filler are included in the model. At the meso-scale a model can only represent a small part of a composite component or article, due to the limitations of computational power and model size. The nodes for the computation can be the meso-scale sub-units instead of a geometric mesh.

Further refinement of scale to the nanometre dimensions brings a model into the molecular domain. In molecular models discrete atomic or in simplified form united atoms are used to build the model. Only a small sub-set of a composite can be modelled because of the complexity of the molecular scale, however discrete chemical properties are represented and assumptions about global properties such as modulus do not need to be made. The properties of the atoms or united atoms are still obtained from sets of parameters that represent the actual molecular properties. These sets of parameters are called force fields, and the values may be derived from actual properties or by ab-initio computational methods from quantum mechanical theory. Application of a suitable force field to the model involves molecular mechanics where the geometries and forces within and between molecules are calculated using Newtonian mechanics, with relationships such as that from Leonard–Jones. Periodic boundary conditions are applied to extend the limited simulation volume to that of a real material (Fig. 23). As an example of this approach, the simulated deformation of a 2D polymer field has been used to calculate a macro-level stress-strain curve, including visualisation of nano-scale void generation, void coalescence and crack formation (Wang, et al, 2003).

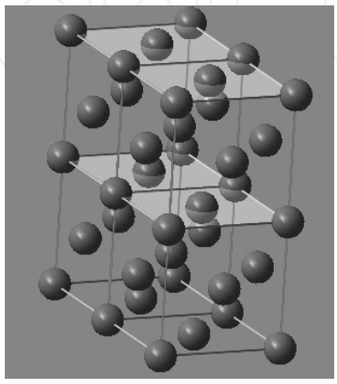

Fig. 23. 3D molecular unit cell model repeatable from each face to create a period boundary system

4. Conclusion

Finite element analysis has provided an implicit means of modelling polymer composites, such as thermoset chopped fibre or woven fabric composites and laminates, thermoplastic–textile and dispersed chopped fibre composites that interprets the stress–strain behaviour in local regions compared with typical volume fraction continuum models. An FEA approach comprising model design, validation, optimisation, simulation and analysis has been described. FEA applied to polymer composites has been reviewed and many examples demonstrated independently using a two-dimensional FEA program. The importance of stress transfer from matrix to fibre is emphasised by stress concentrations. The surface regions and inter-fibre matrix were identified as zones that supported most stress during deformation by bending since one surface is extended while the opposite surface is compressed. Consequently there is a requirement to have fibre rich regions near surfaces and complete compaction, which is readily achieved by a compression moulding process. The interior can be suitably partially compressed to create low density impact resistant composites. A tensile stress gives a uniform deformation field that must be efficiently transferred to the fibres, creating stress concentrations at the fibre–matrix interfaces.

5. References

Ausiello, P., Apicella, A., Davidson, C. L. (2002). Effect of adhesive layer on stress distribution in composite restorations – a 3D finite element analysis, Dental Materials, 18, 295-303.

Beckert, W., Lauke, B. (1995). Fracture mechanics finite element analysis of debonding crack extension for a single fibre pull-out specimen, J. Mat. Sci. Lett., 14, 333-336.

Boisse, P., Borr, M., Buet, K., Cherouat, A. (1997). Finite element simulations of textile composite formed including the biaxial fabric behavior, Comp. B, Eng., 28, 453-464.

Butcher, R. J., Rousseau, C. E., Tippur, H. V. (1999). A functionally graded particulate composite: Preparation, Measurements and failure analysis, Acta Mater. 47, 259-268.

Chang, F. K., Scott, R. A., Springer, G. S. (1982). Strength of mechanically fastened composite joints, J. Comp. Mat. 16, 470-494.

Change, F. K., Chang, K. Y. (1987). A progressive damage model for laminated composites containing stress concentrations, J. Comp. Mat., 21, 834-855.

Chen, X., Liu, Y. (2001). Multiple-cell modelling of fibre-reinforced composites with the presence of interphases using the boundary element method, Comp. Mat. Sci. 21, 86-94.

Choo, H., Bourke, M. A. M., Daymond, M. R. (2001). A finite-element analysis of the inelastic relaxation of thermal residual stress in continuous-fiber-reinforced composites, Comp. Sci. Tech., 61, 1757-1722.

Davies, G. A. O., Zhang, X., Zhou, G., Watson, S. (1994). Numerical modelling of impact damage, Composites, 25, 342-350.

Dehoff, P. H., Anusavice, W. J., Wang, Z. (1995). Three-dimensional finite element analysis of the shear bond test, Dent. Mater., 11, 126-31.

Diaz, J., Romera, L., Hernandez, S., Baldomir, A. (2010). Benchmarking of three-dimensional finite element models of CFRP single-lap bonded joints, Int. J. Adhesion and Adhesives, 30, 178-189.

Dooms, D., Degrande, G., Roeck, G. D., Reynders, E. (2006). Finite element modelling of a silo based experimental nodal analysis, Eng. Structures, 28, 532-542.

Fisher, F. T., Bradshaw, R. D., Brinson, L. C. (2003). Fiber waviness in nanotube-reinforced polymer composites—II: modeling via numerical approximation of the dilute strain concentration tensor, Comp. Sci. Tech., 63, 1705-1722.

Fisher, F. T., Brinson, L. C. (2001). Viscoelastic interphases in polymer-matrix composites: Theoretical models and finite element analysis, Composites Sci. and Tech. 61, 731-748.

Gamble, K., Pilling, M., Wilson, A. (1995). An automated finite element analysis of the initiation and growth of damage in carbon-fibre composite materials, Comp. Structures, 32, 265-274.

Guild, F. J., Young, R. J. (1989). A predictive model for particulate-filled composite materials, J. Mat. Sci., 24, 298-306.

Houshyar, S., Hodzic, A., Shanks, R. A. (2009). Modelling of polypropylene fibre-matrix composites using finite element analysis, eXPRESS Polymer Letters, 3, 2-12.

Houshyar, S., Shanks, R. A. (2003). Morphology, thermal and mechanical properties of poly(propylene) fibre-matrix composites, Macromol. Mat. Eng., 288, 599-606.

Houshyar, S., Shanks, R. A. (2010). Interfacial properties of all-polypropylene composites, e-Polymers, 33, 1-13.

Houshyar, S., Shanks, R. A., Hodzic, A. (2005). The effect of fiber concentration on mechanical and thermal properties of fiber-reinforced polypropylene composites, J. Appl. Polym. Sci., 96, 2260-2272.

Huang A., Bush M. B. (1997). Finite element analysis of mechanical properties in discontinuously reinforced metal matrix composites with ultra fine micro structure. Mat. Sci. Eng. A, 232, 63–72.

Hutchinson, J. W., Jensen, H. M. (1990). Models of fiber debonding and pullout in brittle composites with friction, Mecahnical of Materials, 9,139-163.

Hyung, Y. C., Wu, H. Y. T., Fu-Kuo, C. (1991). A new approach toward understanding damage mechanisms and mechanics of laminated composites due to low-velocity impact. II: analysis, J. Comp. Mat., 25, 1012-1038.

Isakson, G., Levy, A. (1971). Finite element analysis of interlaminar shear in fibrous composites, J. Comp. Mat., 5, 273-276.

Kang G. Z., Gao Q. (2002). Tensile properties of randomly oriented short Al_2O_3 fibre reinforced aluminium alloy composites: II. Finite element analysis for stress transfer, elastic modulus and stress-strain curve. Composites A, Appl. Sci. Manufacturing, 33, 657–667.

Lamkanfi, E., Paepegem, W. V., Degrieck, J., Ramault C. (2010). Strain distribution in cruciform speciments subjected to biaxial loading conditions. Part 1. Two-dimensional finite element model, Polym. Testing, 29, 7-13.

Lee, S. H., Wang, S., Pharr, G. M., Xu, H. (2007). Evaluation of interphase properties in a cellulose fiber-reinforced polypropylene composite by nanoindentation and finite element analysis, Composites A, 38, 1517-1524.

Lim, J. H., Ratnam, M. M., Abdul-Khalil H. P. S (2003). An experimental and finite element analysis of the static deformation of natural fiber-reinforced composite beam, Polym. Testing, 22, 169-177.

Lin, D. X., Ni, R. G., Adams, R. D. (1984). Prediction and measurement of the vibrational damping parameers of carbon and glass fire-reinforced plastics plates, J. Comp. Mat., 18, 132-152.

McCarthy, M. A., McCarthy, C. T. (2002). Finite element analysis of the effects of clearance on single-shear, composite bolted joints, J. Plastics, Rubber Comp., 32, 1-11.

Maligno A. R., Warrior N. A., Long A. C. (2008). Finite element investigations on the microstructure of fibre reinforced composites. Express Polymer Letters, 2, 665–676.

Muheim, D., Griffen, O. H. (1990). 2-D to 3-D global/local finite element analysis of cross-ply composite laminates, J. Reinforced Plastics Comp., 9, 492-502.

Naik, N. K., Shembekar, P. S. (1992). Elastic behaviour of woven fabric composites: I – lamina analysis, J. Comp. Mat.,26, 2196-2225.

Nakamura, T., Imanishi, A., Kashima, H., Ohyama, T., Ishigaki, S. (2001), Stress analysis of metal-free polymer crowns using the three-dimensional finite element method, Int. J. Prosthodont, 14, 401-405.

Nedele, M. R., Wisdom, M. R. (1994). Three-dimensional finite element analysis of the stress concentration at a single break, Comp. Sci. Tech., 51, 517-524.

Pal, P., Ray, C. (2002). Progressive failure analysis of laminated composite plates by finite element method, J. Reiforced Plastics and Composites, 21, 1505-1513.

Pavier, M. J., Clarke, M. P. (1996). Finite element prediction of the post-impact compressive strength of fibre composites, Comp. Structures, 36, 141-153.

Pegoretti, A., Fambri, L., Zappini, G., Bianchetti, M. (2002). Finite element analysis of a glass fibre reinforced composite endoplastic post, Biomaterials, 23, 2667-2682.

Shati F. K., Esat I. I., Bahai H. (2001). FEA modelling of visco-plastic behaviour of metal matrix composites. Finite Elements in Analysis and Design, 37, 263–272.

Song, Y. S., Youn, J. R. (2006). Evaluation of the effective thermal conductivity for carbon nanotube/polymer composites using control volume finite element method, Carbon, 44,710-717.

Soykasap, O. (2010). Finite element analysis of plain weave composites for flexural failure, Polym. Composites, 31, 581-586.

Sun, C. T., Chen, J. K. (1985). On the impact of initially stressed composite laminates, J. Comp. Mat., 19, 490-504.

Tan, P., Tong, L., Steven, G. P. (1998). Modelling approaches for 3D orthogonal woven composites, J. Reinforced Plastics Comp., 17, 545-577.

Taylor, M., Verdonschot, N., Huiskes, R., Zioupos, P. (1999). A combined finite element method and continuum damage mechanicals approach to simulate the in vitro behavior of human cortical bone, J. Mat. Sci.: Mat. In Medicine, 10, 841-846.

Tserpes, K. I., Papanikos, P. (2005). Finite element modeling of single-walled carbon nanotubes, Composites B. Eng., 36, 468-477.

Tsui, C. P., Tang, C. Y., Lee, T. C. (2001). Finite element analysis of polymer composites filled by interphase coated particles, J. Mat. Process. Tech., 117, 105-110.

Vozkova, P.(2009). Elastic modulus FEA modelling of the layered woven composite material, in Petrone, G., Cammarata, G. (editors), Modelling and Simulation, SCIYO Publishing, ISBN 978-3-902613-25-7, p. 651.

Wang, J., Kelly, D., Hillier, W. (2000). Finite element analysis of temperature induced stresses and deformations of polymer composite components, J. Comp. Mat., 34, 1456-1471.

Wang, Y., Sun, C., Sun, X., Hinkley, J., Odegard, G. M., Gates, T. S. (2003). 2-D nano-scale finite element analysis of a polymer field, Comp. Sci. Tech., 63, 1581-1590.

Whitcomb, J. D. (1981). Finite element analysis of instability related delamination growth, J. Comp. Mat., 15, 403-426.

Whitcomb, J., Srinengan, K. (1996). Effect of various approximations on predicated progressive failure in plane weave composites, Comp. Structures, 34, 13-20.

Wisheart, M., Richardson, M. O. W. (1998). The finite element analysis of impact induced delamination in composite materials using a novel interface element, Composites A, 29A, 301-313.

Wisnom, M. R. (2010). Modelling discrete failures in composites with interface elements, Composites A, doi:10.1016/j.compositesa.2010.02.011.

Wong, S., Shanks, R. A., Hodzic, A. (2007). Effect of additives on the interfacial strength of poly(l-lactic acid) and poly(3- hydroxybutyric acid)-flax fibre composites, Comp. Sci. Tech., 67, 2478-2484.

Finite Element Analysis

Edited by David Moratal

ISBN 978-953-307-123-7

Hard cover, 688 pages

Publisher Sciyo

Published online 17, August, 2010

Published in print edition August, 2010

Finite element analysis is an engineering method for the numerical analysis of complex structures. This book provides a bird's eye view on this very broad matter through 27 original and innovative research studies exhibiting various investigation directions. Through its chapters the reader will have access to works related to Biomedical Engineering, Materials Engineering, Process Analysis and Civil Engineering. The text is addressed not only to researchers, but also to professional engineers, engineering lecturers and students seeking to gain a better understanding of where Finite Element Analysis stands today.

How to reference

In order to correctly reference this scholarly work, feel free to copy and paste the following:

Robert Shanks (2010). Modelling of Thermoplastic Fibre-Composites and Finite Element Simulation of Mechanical Properties, Finite Element Analysis, David Moratal (Ed.), ISBN: 978-953-307-123-7, InTech, Available from: http://www.intechopen.com/books/finite-element-analysis/modelling-of-thermoplastic-fibre-composites-and-finite-element-simulation-of-mechanical-properties

INTECH
open science | open minds

InTech Europe
University Campus STeP Ri
Slavka Krautzeka 83/A
51000 Rijeka, Croatia
Phone: +385 (51) 770 447
Fax: +385 (51) 686 166
www.intechopen.com

InTech China
Unit 405, Office Block, Hotel Equatorial Shanghai
No.65, Yan An Road (West), Shanghai, 200040, China
中国上海市延安西路65号上海国际贵都大饭店办公楼405单元
Phone: +86-21-62489820
Fax: +86-21-62489821

IntechOpen